Operational Issues in Solids Processing Plants: Systems View

Christianto Wibowo and Ka M. Ng
Dept. of Chemical Engineering, University of Massachusetts, Amherst, MA 01003

A systematic approach to deal with the operational issues in solids processing plants is presented. Potential problems in various equipment units are identified and classified according to continuum-scale phenomena: breakage, adhesion and cohesion, compaction, bulk solids flow problems, fluid-driven solids flow problems, and segregation. Analysis is performed in the continuum and particle scales so as to identify the causal and opposing effects of each problem. With appropriate mathematical models and empirical correlations, these effects can be related to equipment design, operating conditions, particle attributes, and material properties. The ratio of these competing effects shows whether a potential problem is a real concern and points the direction for taking preventive measures. The action plan may include changing operating conditions or equipment design of a particular unit, or making modifications to upstream equipment units. The method is illustrated with an industrial example: the production of potash.

Introduction

As the chemical processing industries shift from commodity to specialty chemicals, design methods for solids processes which involve steps such as dissolution, crystallization, solid-liquid separation, and bulk solids processing have been receiving considerable attention. A hierarchical procedure that guides the user to generate process alternatives has been developed (Rossiter and Douglas, 1986a,b; Rajagopal et al., 1992). For a selected flowsheet alternative, population balance equations can be used to track the particle-size distribution from unit to unit in a complete plant (Jones, 1984; Barton and Perkins, 1988; Hill and Ng, 1997). Domain-specific synthesis procedures have been developed for crystallization systems (Cisternas and Rudd, 1993; Wibowo and Ng, 2000), crystallizer downstream solid-liquid separations (Chang and Ng, 1998), bulk solids processing (Wibowo and Ng, 1999), as well as crystallization-distillation hybrid systems (Berry and Ng, 1997; Pressly and Ng, 1999).

Despite all of this progress, the present design methods do not address operational problems in a solids processing plant. This is a serious omission because, unlike gas/liquid processes, solids processes are often plagued by operational problems. Indeed, a survey reveals that about 94% of solids plants experienced major performance problems, mostly related to solids flow and handling (Merrow, 1985). Problems such as erratic flow in hoppers, encrustation on equipment walls, vibration in centrifuges, dusting, and insufficient washing of filter cakes can lead to undesirable consequences, including reduced capacity, unsatisfactory product quality, excessive maintenance requirements, equipment malfunction, or even serious safety problems such as fires and explosions.

Fortunately, various problems have been addressed by specialists in particle technology. For example, procedures for properly designing bins, hoppers, and feeders in order to avoid problems such as flow stoppage due to arch formation, have been developed (Johanson, 1992; Carson and Marinelli, 1994). Johanson and Johanson (1988) described means to handle uncontrollable flows caused by fluidization in storage and transportation units. Electrostatic problems in sieving and tabletting were considered by Davies (1991). Pietsch (1996, 1997) discussed how to avoid product quality problems in size enlargement operations, such as the formation of agglomerates with insufficient strength. Moyers (1992) highlighted problems such as encrustation that may arise in the operation of industrial dryers, which he emphasized are strongly influenced by the upstream solid-liquid separation step. Indeed,

Correspondence concerning this article should be addressed to K. M. Ng at the following current address: Dept. of Chemical Engineering, Hong Kong University of Science and Technology, Clear Water Bay, Hong Kong.

an operational problem manifested in one unit can originate in another upstream or downstream unit due to the interconnections among units. This point was reiterated by Chang and Ng (1998) who pointed out that the difficulty in a crystal washing unit is often caused by an excessive amount of fines formed in the upstream crystallizer. Clearly, it is highly desirable to take a systems view of operational issues.

Most of the above-mentioned methods for tackling solids operational problems are based on continuum-scale analyses with phenomenological parameters. For example, the Jenike yield locus gives the stress at which flow is initiated in particulate materials. The permeability characterizes flow through a filter cake. However, considerable effort has also been placed on particle scale analyses. The effect of particle-size distribution on permeability was elucidated by MacDonald et al. (1991). The role of adhesive forces in determining agglomerate strength was considered by Pietsch (1996). Experimental studies indicate that material properties such as the Hamaker constant and dielectric constant, and particle attributes such as morphology and size distribution can be linked to the transport behavior of powders (Lee and Fan, 1993). Molerus (1982) predicted Geldart's powder classification diagram by comparing interparticle cohesion forces and hydrodynamic effects. Since operational problems can often be traced to the particle-level phenomena, a coherent method that considers such problems at both the continuum and particle scales would be beneficial.

This article introduces a procedure in which the effects of material properties, particle attributes, and interparticle forces on powder behavior are taken into account in resolving operational problems in a solids processing plant. While keeping an integral view of the whole process, continuum and particle scale analyses point to the necessary action plan to solve the problem(s) in each equipment unit.

Systematic Method to Resolve Operational Problems in Solids Processing

The method spanning from particle scale to plant scale consists of three steps. In step 1, potential problems classified in terms of the dominant effects or phenomena are identified for each unit using heuristics. In step 2, the causal and opposing effects for each identified phenomenon are compared so as to decide whether the potential problem is likely to be a real concern. In step 3, ways in which the real concerns can be ameliorated or eliminated are identified. Options ranging from merely changing the operating conditions of an equipment unit to installing a new unit are considered. The process alternatives thus generated are evaluated to identify the best candidate for a new plant design or a retrofit.

The overall strategy of this method is as follows. Clearly, whether operational problems in a solids processing unit occurs or not depends on both the equipment and the material it handles. Figure 1 depicts the way in which the material and equipment (boxes on top row) interact with each other. The material is characterized by its intrinsic properties such as Hamaker constant and Young's modulus, as well as particle attributes such as particle-size distribution (PSD) and shape. The equipment is characterized by its design, as well as the operating conditions. Thus, the bulk properties of the solids (lefthand side box, second row) are determined by both mate-

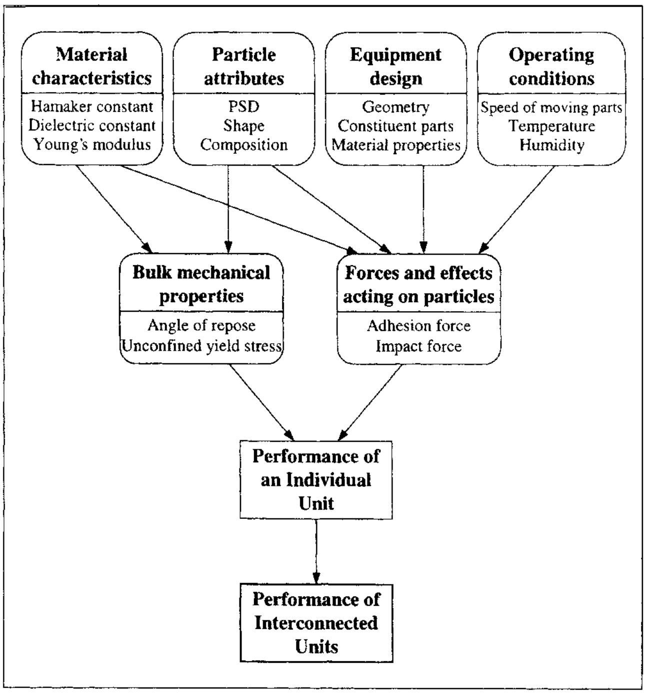

Figure 1. Interrelationships of factors affecting the performance of a solids processing unit.

rial properties and particle attributes. For example, the effective angle of internal friction of a powder depends on the Hamaker constant, the PSD, and so on. The forces and effects acting on the particles (righthand side box, second row) depend on the particle characteristics, as well as the environment imposed by the processing unit. For example, adhesion of a particle to an equipment wall is influenced by the Hamaker constants of the material and the wall. Also, whether breakage occurs depends in part on the particle fracture energy and the speed of the moving parts within the equipment. In other words, the potential operability issues of an individual equipment item (box on third row) are identified by examining the various forces and effects acting on the bulk solids, as well as their responses, which in turn depend on the material and equipment. Based on the results of this analysis, as well as an examination of upstream and downstream units, proper actions can be taken to tackle the roots of the potential problems.

Step 1: Identification of Potential Problems

Figure 2 shows some generic problems commonly encountered in solids processing plants. Impact can cause *breakage* (Figure 2a). Particles bouncing along a wall can result in *attrition* (Figure 2b). *Adhesion* of particles to a wall may cause the formation of a layer of deposited solids (Figure 2c). They can also form aggregates due to *cohesion* (Figure 2d). When a bed of bulk solids is subjected to a compressive pressure, *compaction* may occur (Figure 2e). A stable arch may form due to the adhesion forces between particles near a hopper outlet, causing *flow stoppage* (Figure 2f). Another problem related to a hopper is funnel-flow, where some material near the wall is stagnant, while those at the center flows in a fun-

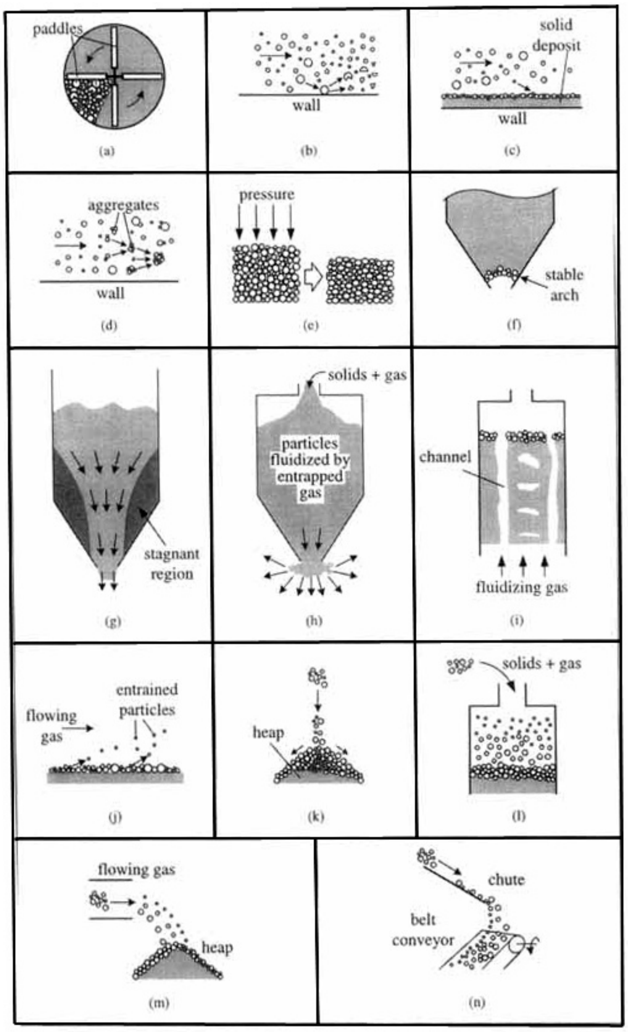

Figure 2. Pictorial representation of operational problems in solids processing.

Shaded regions represent particles.

nel-shaped channel (Figure 2g). A fluid-driven solids flow problem may occur when air is entrapped inside a bin, causing fluidization of the contents (Figure 2h). This leads to uncontrollable *flooding*, where as indicated by the multiple arrows the entire content of the hopper is emptied just in several seconds. In a fluidized bed, *gas channeling* may occur (Figure 2i). Another type of fluid-driven solids flow is the *entrainment* of small particles exposed to a flowing gas (Figure 2j). Segregation takes place through different mechanisms. In percolation, small particles move through the pores between larger particles (Johanson, 1987). When particles are poured onto a heap, smaller particles tend to concentrate at the center while larger particles move aside to the peripherals of the heap (Figure 2k). *Elutriation* occurs because particles of different sizes have different settling velocities. When they are poured into a bin, small particles tend to float and later settle on top of the larger ones (Figure 2l). In *trajectory segregation*, smaller particles tend to travel farther and concentrate on the far side of the heap (Figure 2m). *Friction segregation* occurs with particles having different frictional resistances (Carson et al., 1986). Upon leaving an inclined chute, smaller particles (or particles with higher frictional angle) tend to concentrate on the side closer to the chute. This may lead to undesired classification in a belt conveyor receiving the particles (Figure 2n).

Common problems in solids processing units, classified according to the relevant continuum-scale phenomena, are given in Table 1. Maintenance-related problems such as corrosion and equipment wear are not considered. Operational problems related to the particle-size distribution (PSD) or the crystallization unit, which require a different analysis, are also excluded. The same generic problem can appear in several unit operations, but may have different symptoms and consequences. For example, breakage in a fluidized-bed dryer may cause entrainment problems. A similar problem in a filter leads to a low cake porosity, which in turn causes a reduction in filtration rate. Table 1 can be used to identify potential problems in each unit as well as the relevant continuum-scale phenomena. Sometimes, two or more phenomena may be responsible for the occurrence of a particular problem. For example, low cake porosity in a filter can be a result of either particle breakage or compaction due to the compressive pressure on the cake. In such a case, the analysis must include all relevant phenomena.

Step 2: Comparison of Competing Effects

For each phenomenon relevant to the problem on hand, we identify the *causal effect* (CE), which is responsible for its occurrence, as well as the *opposing effect* (OE), which counters the action of *CE*. Table 2 lists the *CE* and *OE* for continuum-scale phenomena relevant to solids processing. These effects are related to the forces acting on the particles, the material properties, and particle attributes. Comparison of these competing effects can reveal which effect is dominant, and, therefore, leads to the prediction of whether or not a problem may occur in a particular situation. For example, whether a particle breaks depends on the applied stress and tensile strength, as well as the presence of cracks due to previous processing steps. A particle adheres to the equipment wall if the adhesion force exceeds that of the forces separating them. Some important material properties in particle technology such as strength, hardness, and toughness are listed in Table 3 along with their representative parameters. To illustrate the forces that may be present, Figure 3 shows four typical situations in solids processing. The relevant basic forces and equations for their estimation are listed in Table 4.

Figure 3a shows a sphere moving in a fluid. Equations 1 and 2 provide an estimation of the gravity-buoyancy and drag forces. Figure 3b shows a sphere close to a wall, whereas Figure 3c shows two spheres in close proximity. The van der Waals force is the main attractive force between them. As Eqs. 3 and 6 indicate, its magnitude depends on the Hamaker constant, particle size, and separation distance (z). The effect of the van der Waals force is felt only when the objects are sufficiently close on the order of about 1 nm (Visser, 1989). When two particles are in contact, the separation distance can be arbitrarily taken as $z_0 = 4$ Å (Dahneke, 1971). The same assumption can be applied for soft material, as in-

Table 1. Common Problems in Solids Processing Units, Classified According to Continuum-Scale Phenomena

Continuum-Scale Phenomena and Generic Problems	Unit Operation							
	Solids Mixing	Solid/Fluid Separation	Drying	Classification	Size Reduction	Size Enlargement	Storage	Transportation
Breakage								
• Due to applied pressure (Fig. 2a)	1	2	—	—	3	—	—	—
• Due to attrition (Fig. 2b)	4	—	—	—	3	—	5	6
Adhesion and cohesion								
• Deposition/encrustation (Fig. 2c)	7	—	8	9	10	—	—	11
• Formation of aggregates (Fig. 2d)	—	—	12	13	—	14	15	16
Compaction								
• Compaction (Fig. 2e)	—	17	—	—	—	18	19	—
Bulk solids flow problems								
• Arch formation (Fig. 2f)	—	—	—	—	—	—	20	—
• Funnel flow (Fig. 2g)	—	—	—	—	—	—	21	—
Fluid-driven solids flow problems								
• Flushing flow (Fig. 2h)	—	—	—	—	—	—	22	23
• Erratic fluidization (Fig. 2i)	24	—	25	—	—	26	—	—
• Entrainment (Fig. 2j)	—	—	27	28	—	—	—	29
Segregation								
• Sifting (Fig. 2k)	—	—	—	30	—	—	31	—
• Elutriation (Fig. 2l)	32	—	—	—	—	—	31	—
• Trajectory segregation (Fig. 2m)	—	—	—	—	—	—	—	33
• Friction segregation (Fig. 2n)	—	—	—	—	—	—	—	34

Examples of Specific Problems

1. Undesired change in output PSD in mixer with paddles
2. Low cake porosity and permeability due to formation of fines, leading to reduced filtration rate
3. Insufficient or excessive breakage, leading to a product having undesired PSD
4. Undesired change in output PSD in a fluidized-bed mixer
5. Generation of fines near rough walls, leading to a undesired PSD
6. Generation of fines during pneumatic conveying, leading to dusting and undesired PSD
7. Encrustation on tumble mixer walls, leading to the need for cleanup
8. Encrustation in a rotary dryer, leading to reduced capacity and the need for cleanup
9. Sticking of particles on screen wires, causing screen blinding
10. Deposition of relatively soft solids particles on the balls in a ball mill, leading to decreasing milling efficiency
11. Solids deposition on pneumatic conveyor walls, leading to plugging on the line
12. Change in PSD of the dried material
13. Formation of temporary aggregates, such as that caused by electrostatic forces, leading to reduced screen efficiency
14. The product PSD in a pan or drum granulator does not meet the desired specification
15. Formation of crust or large particles blocking the outlet
16. Aggregate formation during pneumatic conveying, leading to a change in PSD
17. Low cake porosity and permeability due to compaction of filter cake in a centrifugal filter, leading to reduced filtration rate
18. Formation of agglomerates with insufficient strength
19. Compaction of material in the bottom part of the bin, leading to arch formation
20. Formation of a stable arch blocking a hopper outlet, causing flow stoppage
21. Formation of a stagnant region, leading to reduced capacity and fire and explosion hazard when handling combustible material
22. Spillage of valuable materials, leading to product loss and need for costly cleanup
23. Spillage and dusting in screw conveyors due to entrapment of compressed air, leading to product loss and need for cleanup
24. Formation of stagnant region in a fluidized-bed mixer, leading to incomplete mixing
25. Channeling in fluidized-bed dryer, leading to insufficient drying
26. Channeling in fluidized-bed granulator, leading to undesired product PSD
27. Entrainment of small particles by flowing air in rotary dryer
28. Dusting during screening due to air turbulence
29. Dusting in belt conveyors due to air turbulence
30. Loss of undersized particles to product stream in a vibrating screen
31. In-bin segregation, leading to product nonuniformity when the content of the bin is discharged
32. Demixing during emptying of a batch tumble mixer, leading to nonuniform product
33. Concentration of small particles on one side of a bin receiving feed horizontally from a pneumatic conveying line
34. Concentration of small particles on one side of a conveyor belt receiving feed from an inclined chute

dicated by Eq. 7. Because of its short length of influence, the van der Waals force is significantly affected by surface roughness. For rough particles, it is the surface asperity that is actually in contact with another surface. Consequently, the van der Waals force in this case should be calculated based on the size of the asperity, which can be approximated by multi-

Table 2. Causal and Opposing Effects for the Phenomena in Solids Processing

Phenomena	Causal Effect (CE)	Opposing Effect (OE)
Breakage	Applied stress or shear	Tensile strength
Adhesion and cohesion	Adhesive effects	Separating effects
Compaction	Applied pressure	Yield strength
Bulk solids flow	Applied stress	Cohesive strength
Fluid-driven solids flow	Drag forces	Gravity and adhesive forces
Segregation	Bulk motion	Uniformity

plying d_p with a factor of order 10^{-1} for micron-sized particles (Krupp, 1967). Electrostatic force (Eqs. 4 and 8) exists when the particles are charged. Triboelectrification or particle self-charging due to friction is a common phenomenon in a system of flowing dry bulk solids. In such a case, the maximum magnitude of the electrostatic force can be estimated using Eq. 5. Since the electrostatic force generated by triboelectrification has only a temporary effect, it is only important if the relaxation time is greater than the processing time (Bailey, 1984). The relaxation time, defined as the duration of time during which 63.2% of the original charge dissipates

Table 3. Mechanical Properties of Materials (van Vlack, 1980)

Property and Definition	Representative Parameter	Symbol	Unit
Maximum strength (resistance to failure)	Tensile strength	σ_t	Pa
Hardness (resistance to initial deformation or indentation)	Yield strength	σ_y	Pa
Toughness (energy for failure by fracture)	Fracture energy	γ_f	$J \cdot m^{-2}$
Elasticity (ratio of applied normal stress and elastic strain)	Young's modulus	E	Pa
Ratio of applied shear stress and shear strain	Shear modulus	G	Pa
Ductility (plastic strain at failure)	Failure elongation	e_f	Dimensionless

Table 4. Equations for Estimating Basic Forces in Some Representative Situations

Situation / Equation	Eq.	Reference
A single sphere on air (Figure 3a)		
Gravity-buoyancy force		
$W - F_B = \frac{\pi}{6} d_p^3 (\rho_S - \rho_F) g$	(1)	
Drag force		
$F_D = \left(\frac{\pi}{4} d_p^2\right) \frac{\rho_F}{2} v_p^2 f(N_{Re})$	(2)	Bird et al. (1960)
A sphere and a wall (Figure 3b)		
van der Waals force		
$F_{vdW} = \frac{A d_p}{24 z^2}$	(3)	Visser (1989)
Electrostatic force (general)		
$F_E = \frac{q^2}{16 \pi \epsilon_0 z^2}$	(4)	Bailey (1984)
Electrostatic force (charging by triboeletrification)		
$F_{E,\max} = 79.2(\pi d_p^2)\left(\frac{3\epsilon_r}{\epsilon_r + 2}\right)$	(5)	Lee and Fan (1993)
Two identical spheres (Figure 3c)		
van der Waals force (rigid spheres)		
$F_{vdW} = \frac{A d_p}{12 z^2}$	(6)	Visser (1989)
van der Waals force (deformable spheres in contact)		
$F_{vdW} = \frac{A d_p}{12 z_0^2}\left(1 + \frac{A}{6\pi z_0^3 H}\right)$	(7)	Dahneke (1972)
Electrostatic force		
$F_E = \frac{q^2}{16 \pi \epsilon_0 z^2}\left(1 - \frac{2z}{\sqrt{d_p^2 + 4z^2}}\right)$	(8)	Bailey (1984)
Two identical spheres with a liquid bridge (Figure 3d)		
Capillary force		
$F_C = \frac{\pi d_p \gamma \cos\theta}{1 + \tan\left(\frac{\psi}{2}\right)}$	(9)	Visser (1976)

due to redistribution, is given by

$$t_r = \Omega \epsilon_r \epsilon_0 \quad (10)$$

where Ω is the specific resistivity of the particle in ohm·m. Figure 3d shows the situation where a liquid is present in the system. Equation 9 estimates the capillary force acting on the wetted surface, due to the presence of a liquid bridge connecting the particles.

Semi-quantitative approach

The competing effects are compared in a systematic manner by defining a dimensionless group to represent their relative magnitudes. When the value of this dimensionless number exceeds a limiting value N^*, the causal effect is likely to occur. In other words, the criterion for occurrence is in the form of

$$\frac{CE}{OE} \geq N^*. \quad (11)$$

Obviously, the value of N^* depends on material properties, equipment settings, and operating conditions. The time effect of the process must be taken into account in the analysis, because many units in solids processing undergo batch, semi-batch, or cyclic operation. The worst conditions, such as maximum load or maximum water content, need to be identified since they determine the extreme values of CE and OE.

For situations that are difficult to describe mathematically, such as segregation, a quantitative analysis cannot be performed in a meaningful way. Instead of dimensionless numbers, we use heuristics to identify whether segregation may be an issue. In fact, there exist heuristics for other phenomena, which can be used to quickly identify problems in typical situations (Table 5).

Table 5. Heuristics for Identifying Whether Operational Problems are Likely to Occur

General Heuristics
- In assessing a potential operational problem, always consider how operating conditions change over time.
- The relative magnitude of the electrostatic force generated by triboelectrification with respect to its maximum value (Eq. 5) is about 8% for solids flow, and about 60% for pneumatic conveying and compaction (Eichel, 1967).
- Generally, powders are capable of retaining the charge generated by triboelectrification if the resistivity of the material is above 10^9 ohm·m (Davies, 1991).
- Capillary force is usually dominant if the degree of saturation (volume fraction of pores filled with liquid) is between 0.4 to 0.8 (Schubert, 1984).
- Adhesion forces can increase during storage or transportation due to an increase in moisture content, if the material is hygroscopic and the environment is not moisture-free.

Heuristics Related to Solids Flow
- Bulk solids residing in a bin without moving for an extended time may exhibit increased cohesiveness due to compaction, crystallization, reaction, or adhesive bonding (Carson and Marinelli, 1994)

Heuristics Related to Breakage
- Breakage of brittle materials due to attrition is likely to occur during dilute-phase pneumatic conveying.
- Breakage of brittle particles may occur if they slide against a rough wall during mass flow inside a hopper (Johanson, 1987).
- Energy loss due to abrasion and particle deformation during breakage can lead to heat accumulation in a size reduction unit (Hixon, 1991).

Heuristics Related to Compaction
- Compaction can occur to the material in the bottom part of storage units due to the pressure generated by the material above it.
- If there are problems related to low filter cake porosity, consider the possibility of compaction due to the absence of fluid in the pores.
- Entrapment of air in a roller compactor may occur if the roller speed at the tip is above 0.2–1.5 m/s (Sommer, 1988; Pietsch, 1997).

Heuristics Related to Fluidization
- Entrainment due to turbulent gas flow is likely to occur if the particles are smaller than 50 μm in size.
- Fluidization in storage bins is likely to occur if the feed is rapidly introduced at the top of the bin in the vertical direction coming from a vertical, centrally-located pneumatic conveying line (Johanson, 1987).
- Fluidization in storage bins due to entrapment of air is likely if the bottom of the vessel is sealed and connected to another unit (such as a screw conveyor) (Johanson and Johanson, 1988).

Heuristics Related to Segregation
- Segregation is not a serious problem if all the particles are smaller than 30 μm or if they are slightly moist (Williams, 1990).
- Segregation due to percolation is likely to be of concern if particles of different density or size are poured into a heap or let slide on an inclined chute (Carson et al., 1986; Williams, 1990).
- The tendency of segregation of binary mixtures due to percolation decreases substantially if the ratio of particle diameters is lower than 1.3 (Carson et al., 1986).
- Segregation during emptying of a storage unit is accentuated when funnel flow occurs (Johanson, 1978, 1987).
- Segregation is likely to occur in a fluidized bed if the particles being processed are of different density or size.

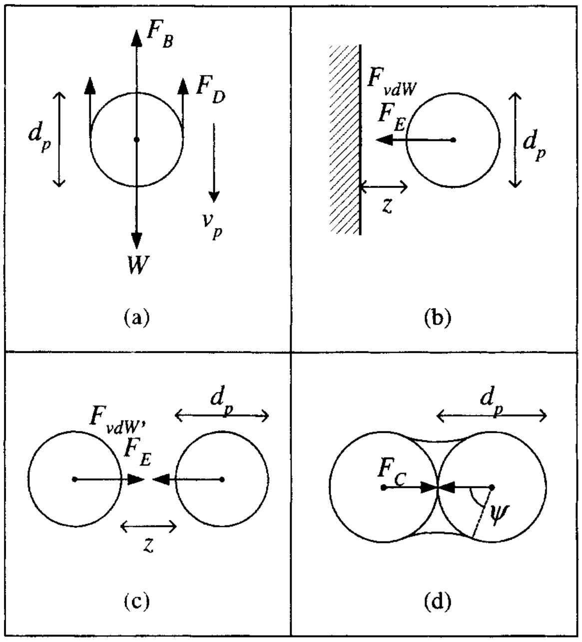

Figure 3. Various situations considered in Table 4.

(a) Single sphere; (b) sphere near a wall; (c) two identical spheres; (d) two spheres with a liquid bridge.

To illustrate this approach, eight commonly encountered problems in solids processing are considered (Figure 4). Table 6 summarizes the dimensionless numbers used in each situation, along with theoretical predictions for N^*. Some situations are discussed in more detail below.

Breakage Number. We consider here the potential problem of particle breakage due to applied stress (Figure 4a) and as a result of particle impact on a surface (Figure 4b). Breakage occurs if the applied stress on a particle σ_c exceeds its strength σ_t, the ratio of which is expressed by the breakage number defined in Eq. 12. For breakage caused by pressure, σ_c can be approximated by taking d_p^2 as a representative area on which a force F_P is applied. For breakage as a result of particle impact on a surface, σ_c can be approximated as (Stuart-Dick and Royal, 1992)

$$\sigma_c = \rho_b v_1^2 \sin^2 \theta. \tag{26}$$

The limiting breakage number (N_{Br}^*) in Eq. 13 is found by solving an equation proposed by Kendall (1978) for estimating the necessary stress to cause breakage of an ideal-shaped specimen. This number is a function of material properties represented by the brittleness index, N_{BI} (Eq. 14), which compares resistance to deformation with the resistance to fracture. Similar brittleness indices have been reported in the

Table 6. Dimensionless Numbers Used in Commonly Encountered Situations in Solids Processing and Their Limiting Values

Phenomenon or Situation	Dimensionless Number Representing CE/OE		Limiting Value	
Breakage by applied pressure (Figure 4a) Breakage by impact (Figure 4b)	Breakage number $N_{Br} = \frac{\sigma_c}{\sigma_t}$	(12)	$N_{Br}^* = \frac{1}{2} - \frac{1}{2}\sqrt{1 - 4(N_{BI})^{-1/2}}$	(13)
			where $N_{BI} = \frac{3\sigma_t^2 d_p}{2E\gamma_f}$	(14)
Encrustation on equipment wall (Figure 4c) Aggregation of dry particles (Figure 4d)	Adhesion number $N_{Ad} = \frac{F_{adh}}{F_{sep}}$	(15)	$N_{Ad}^* = 1$	(16)
Agglomeration due to the presence of liquid (Figure 4e)	Adhesion number $N_{Ad} = \frac{\mu}{4\rho_S d_p u_0}$	(17)	$N_{Ad}^* = \left[\left(1 + \frac{1}{e}\right)\ln\left(\frac{\delta}{r}\right)\right]^{-1}$	(18)
Compaction (Figure 4f)	Compaction number $N_{Co} = \frac{\sigma_c}{\sigma_y}$	(19)	$N_{Co}^* = \frac{1}{k\sigma_y(1-\epsilon)} \ln \left(\frac{\frac{\sigma_{t,\max}}{\sigma_y} - N_{SI}}{\frac{\sigma_{t,\max}}{\sigma_y} - N_{SI,0}} \right)$	(20)
			where $N_{SI} = \frac{1-\epsilon}{\epsilon} \cdot \frac{F_{adh}}{\sigma_y d_p^2}$	(21)
Bulk solids flow from a hopper (Figure 4g)	Flow number $N_{Fw} = \frac{\rho_s g D_o d_p^2 \epsilon}{F_{adh}}$	(22)	$N_{Fw}^* = N_{Fw}^*(\phi, \phi_w, \beta)$	(23)
Entrainment and fluidization behavior (Figure 4h)	Fluidization number $N_{Fl} = \frac{F_D}{W - F_B}$	(24)	$N_{Fl}^* = 1$	(25)

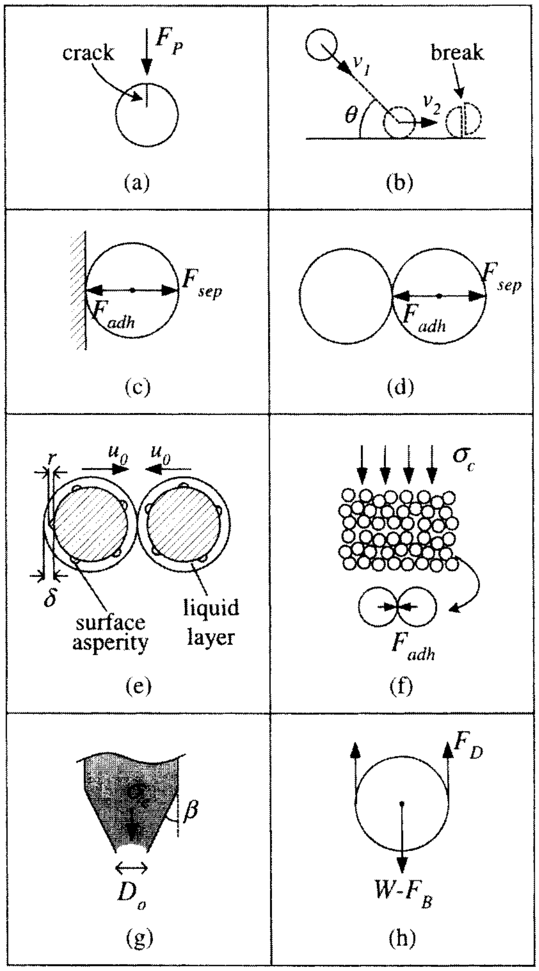

Figure 4. Various situations considered in Table 6.

(a) Particle under compressive stress; (b) particle impacting a surface; (c) particle sticking on a surface; (d) particles forming an aggregate; (e) agglomeration of particles in the presence of liquid layers; (f) compressed body of bulk solids; (g) hopper outlet; (h) particle in a flowing fluid.

literature, as summarized by Quinn and Quinn (1997). A high N_{BI} indicates that the material is more apt to fracture than deform. If N_{BI} is low, the material is more resistant to fracture, because any applied stress is distributed through deformation. In other words, the material appears plastic rather than brittle. Kendall (1978) reported a critical value of particle size below which breakage is impossible. This corresponds to $N_{BI} = 16$, below which Eq. 13 has no solution.

Adhesion Number. Figure 4c illustrates a particle adhering to the equipment wall, a situation that can lead to encrustation. This situation occurs when the adhesion forces exceed the separating forces. Adhesion forces include the van der Waals force (Eq. 3), electrostatic force (Eqs. 4 and 5), or capillary force (Eq. 9), among others. Although several forces can act simultaneously, it is often the case that only one is dominant whereas others are negligible. For example, when handling insulating materials, the electrostatic force generated by triboelectrification is often the dominant adhesion force. If liquid is present, the capillary force is usually dominant. The separating force can be gravity or drag forces. The adhesion number, defined as the ratio of the adhesion force to the separating force (Eq. 15), must exceed unity for adhesion to occur.

Another common problem during powder handling is aggregation (Figure 4d). Although aggregation is often caused by partial dissolution and resolidification of the solid in the presence of moisture, dry powder can also aggregate due to adhesion forces. Similar to the encrustation problem, we assess the importance of these forces by comparing them with the separation forces.

Contrary to the handling of dry particles, aggregation is the desired outcome in tumble agglomeration units such as a pan or drum granulator. In such a unit, a viscous liquid is often used as a binder to promote coalescence of particles. Figure 4e depicts a situation where two particles, each surrounded by a liquid layer, approach each other with a velocity u_0. When the two particles collide, a liquid bridge will form. The collision causes the particles to recoil, but the viscous liquid restricts the movement of the particles. If the rebound velocity is not sufficiently high, the liquid bridge between the particles keeps them together, and agglomeration occurs. In such a dynamic system, the Young-Laplace equation for estimating the capillary pressure is not applicable; instead, viscous forces should be considered as the adhesive effect (Ennis et al., 1991; Tardos, 1998). The opposing effect is the rebound velocity, which can be related to the initial velocity of the particles prior to collision. Comparing these two effects leads to the adhesion number in Eq. 17, which is the reciprocal of the Stokes number defined in Ennis' work. A rough estimate for the critical value of this number is given in Eq. 18.

Compaction Number. In pressure agglomeration, a mass of powder is shaped and densified by applying a compressive pressure (Figure 4f). This compression leads to the reduction of porosity and strengthening of cohesion forces between particles. We define the compaction number N_{Co} as the ratio of the applied compressive pressure to the yield strength of the material (Eq. 19). The critical compaction number (N_{Co}^*) in Eq. 20 gives an estimate of the necessary pressure to form a body with a certain strength. If the compressive pressure is less than what is required, the formed body will lack strength and may break undesirably during subsequent handling. Equation 20 is a dimensionless form of the Leuenberger's equation, which is in good agreement with experimental data (Sommer, 1988). $\sigma_{t,\max}$ is the tensile strength of the body at a fully compressed condition ($\epsilon = 0$). The strength index N_{SI} represents the desired tensile strength of the resulting body. According to Rumpf (1970), it depends on the porosity (ϵ), particle diameter (d_p), and adhesion forces that bind the particles together, as shown in Eq. 21. Here, the van der Waals force is the primary adhesion force.

Flow Number. Figure 4g depicts a column of bulk solids inside a hopper. According to Jenike (1964), flow stoppage occurs when the applied stress on the column is less than its cohesive strength. The applied stress is proportional to the compacting stress under which the column was formed. The inverse of this proportionality constant is known as the flow factor (*ff*), and its value depends on the material as well as the hopper. The compacting stress acting on the particles at the bottom of the hopper is the pressure exerted by the weight of the particles above them, after subtracting out the effect of wall friction. Based on a force balance on a slice of bulk solids in the hopper, Janssen (1895) showed that the vertical pressure p_v exerted on the particles in the hopper can be estimated by solving

$$\frac{dp_v}{dh} = \rho_b g - \frac{4kp_v(\sin\beta + \mu_w \cos\beta)}{D(h,\beta)} \tag{27}$$

where ρ_b is the bulk density, μ_w is the coefficient of wall friction, and D is the hopper diameter, which varies with height in the conical section. In this equation, k is the proportionality constant between the radial and vertical pressures, known as the Janssen constant. Equation 27 is difficult to solve analytically, but assuming β is small and $D \ll h$, it is possible to write the solution in a simple form

$$p_v = \rho_b g D_o f(\phi_w, \beta) \tag{28}$$

where D_o is the diameter of the hopper outlet and ϕ_w ($= \tan^{-1}\mu_w$) is the angle of wall friction. Finally, the applied stress can be related to p_v as

$$\sigma_c = \frac{1}{ff(\phi,\phi_w,\beta)} \cdot \rho_b g D_o f(\phi_w,\beta). \tag{29}$$

The cohesive strength can be represented by the unconfined yield stress, which is the major principal stress needed to cause the column to collapse. Its value depends on material properties, as well as the compacting stress. Molerus (1978) proposed that the unconfined yield stress of the powder can be estimated using the expression

$$f_c = \frac{2\sin\phi}{1-\sin\phi} \cdot \frac{1-\epsilon}{\epsilon} \cdot \frac{F_{\text{adh}}}{d_p^2}. \tag{30}$$

The major adhesion force is typically the van der Waals force, but capillary force may also be present if the powder is moist.

Substituting Eqs. 29 and 30 to Jenike's criterion, $\sigma_c/f_c \geq 1$, and noting that $\rho_b = \rho_s(1-\epsilon)$, we obtain a criterion for bulk solids flow from a hopper, which can be written as

$$N_{Fw} \geq N_{Fw}^*(\phi, \phi_w, \beta) \tag{31}$$

where the flow number N_{Fw} is defined by Eq. 22. This expression is in agreement with Jenike's relationship for the minimum hopper outlet diameter (Jenike, 1964). The critical value $N_{Fw}{}^*$ can be found from charts provided by experts in hopper design, available in various texts (Woodcock and Mason, 1987; Williams, 1990; Tardos, 1999). When the flow number is below this critical value, flow problems such as arch formation and rat-holing may be encountered.

Fluidization Number. Here we consider a particle in contact with a flowing fluid, as illustrated in Figure 4h. When the drag force acting on the particle exceeds the gravity-buoyancy force (Eq. 1), the particle will be carried away by the flow, creating an entrainment problem. The ratio of the drag force to the gravity-buoyancy force is expressed by the fluidization number, the value of which must exceed unity for entrainment to occur. The fluid flow may be a result of forced convection, such as in a fluidized bed, or air turbulence, such as in an open conveyor. Substituting Eqs. 1 and 2 into Eq. 26, we obtain

$$N_{Fl} = \frac{F_D}{W - F_B} = \frac{3\rho_F v_F f(N_{Re})}{4(\rho_S - \rho_F) g d_p}. \tag{32}$$

When ρ_S and ρ_F are 2,000 and 1.3 kg·m^{-3}, respectively, a simple calculation reveals that particles smaller than 50 μm in diameter are easily carried away even by turbulent air ($v_F = 0.1$ m/s).

Molerus (1982) showed that a similar analysis can be used to predict the fluidization behavior of bulk solids, according to Geldart's (1973) classification. The powder is likely to exhibit a certain behavior when the value of the fluidization number falls within a particular range. For example, group A behavior (aeratable) is observed when the drag force overcomes the adhesive force between particles, causing breakup of the fixed-bed structure. Assuming van der Waals force to be the dominating force, the fluidization number is defined as

$$N_{Fl} = \frac{3\pi\rho_F v_F^2 d_p f(N_{Re}) z_0^2}{A}. \tag{33}$$

Molerus proposed a lower limit of about 10^{-3}, below which the powder exhibits group C behavior (cohesive).

Parameter estimation

To complete the analysis, the quantities appearing in the relevant dimensionless numbers must be estimated. This requires values of parameters such as the Hamaker constant, dielectric constant, and so on. In the absence of experimental data, order-of-magnitude estimates are often useful. Table 7 gives typical values of some relevant parameters. If time permits and resources are available, a more accurate value can be obtained from measurements of the parameter or property. Table 8 lists some standard methods for such measurements. If necessary, bulk solids attributes can also be estimated using empirical models. For example, a model for estimating the porosity of a bed of spheres from the PSD has been proposed by Ouchiyama and Tanaka (1984). Recently, Rouault and Assouline (1998) proposed a probabilistic approach to determine the pore-size distribution of a bulk powder and the interconnectivity among the pores.

Material properties may change during processing, often because of moisture adsorption or chemical transformation. Such a change becomes particularly important and needs special attention if hygroscopic or degradable materials are involved. When particles adsorb moisture, the van der Waals force decreases significantly due to the change in Hamaker constant (Visser, 1989)

$$A_{SL} = \left(\sqrt{A_S} - \sqrt{A_L}\right)^2 \tag{34}$$

where the subscripts S, L, and SL refer to the solid in vacuum, the liquid, and the solid in the presence of the liquid, respectively. On the other hand, the electrostatic force increases (Tombs, 1995). If the surface of a particle is covered

Table 7. Typical Values of Relevant Parameters Representing Material Properties

Parameter	Units	Range of Value		Ref.
Tensile strength σ_t	MPa	Metals	200–2,500	Ashby and Jones (1980)
		Polymers	1–100	
		Ceramics	low	
		Composites	4–2,000	
Yield strength σ_y	MPa	Ice	85	Ashby and Jones (1980); Shackelford (1992)
		Metals	100–2,000	
		Ceramics	2,000–10,000	
		Polymers	1–100	
		Composites	4–2,000	
Failure energy γ_f	$J \cdot m^{-2}$	Ice	3	Ashby and Jones (1980); Schönert (1972)
		Metals	10^3–10^6	
		Ceramics	10^1–10^2	
		Polymers	10^2–10^4	
		Composites	10^3–10^5	
Young's modulus E	MPa	Ice	9.1×10^3	Ashby and Jones (1980); van Vlack (1980)
		Metals	1.4×10^4–2×10^5	
		Ceramics	2×10^5–3.5×10^5	
		Polymers	10^2–10^4	
		Composites	10^3–10^5	
Hamaker constant A	$J/10^{20}$	Water	4.38	Dahneke (1972); Visser (1972)
		Polymers	6–9	
		Ionic crystals	6–15	
		Oxides	10–16	
		Metals	16–46	
		Hydrocarbons	4.6–10	
Dielectric constant ϵ_r	—	Water	78.4	Young and Frederikse (1973)
		Polymers	2–9	
		Ionic crystals	5–10	
		Oxides	9–14	
		Metals	10–400	
Electrical resistivity Ω	ohm·m	Water	1.82×10^5	Eichel (1967); Bailey (1984); Lide (1997)
		Metals	10^8	
		Polymers	10^{13}–10^{15}	
		Organic liquids	$3\times10^3-10^{16}$	
Surface tension γ	$N \cdot m^{-1}$	Water	0.073	Nelson (1988)
		Metals	1–2	
		Metal oxides	0.1	
		Hydrocarbons	0.02–0.03	

by a liquid layer with thickness δ, the dielectric constant can be approximated by

$$\epsilon_{r,SL} = \epsilon_{r,L}\left[\frac{\left(\dfrac{d_p+\delta/2}{d_p}\right)^3 + 2\left(\dfrac{\epsilon_{r,S}-\epsilon_{r,L}}{\epsilon_{r,S}+2\epsilon_{r,L}}\right)}{\left(\dfrac{d_p+\delta/2}{d_p}\right)^3 - \left(\dfrac{\epsilon_{r,S}-\epsilon_{r,L}}{\epsilon_{r,S}+2\epsilon_{r,L}}\right)}\right] \quad (35)$$

It is important to note that moisture adsorption may also affect the relative importance of the forces acting on a particle, owing to the capillary force in the presence of a liquid bridge.

Step 3: Generation of Alternative Solutions

The final step is to identify possible solutions to minimize or, if possible, completely avoid the occurrence of the problem. Naturally, this can be achieved by eliminating or reducing the causal effect, or by increasing the opposing effect.

Table 8. Standard Methods for Measurement of Bulk Solids and Material Properties

Parameter	Method	Ref.
Tensile strength, σ_t	Tensile test	Ashby and Jones (1980)
Hardness,* H	Brinell test, Rockwell test, Vickers test	van Vlack (1980)
Fracture energy, γ_f	Charpy test, Izod test	van Vlack (1980)
Young's modulus, E	Sound velocity measurement	Ashby and Jones (1980)
Hamaker constant, A	Refractive index measurement	Lee and Fan (1993)
Dielectric constant, ϵ_r	Capacitance measurement	Young and Frederikse (1973)
Unconfined yield stress	Jenike's shear test	Jenike (1964)
Segregation potential	Sifting-segregation test, fluidization-segregation test	Carson and Marinelli (1994)

*Related to yield strength by the relationship $H = 3\sigma_y$ (Ashby and Jones, 1980).

Table 9. Recommended Actions to Resolve Operational Problems in Solids Processing

Quantity to be Modified	Actions Concerning the Individual Unit	Actions Concerning Upstream Units
Particle Attributes		
Particle size	None	Manipulate particle formation stage Manipulate breakage and agglomeration in preceding units
Bulk porosity	Avoid compaction by using lower height to diameter ratio (in storage bins) Provide a means and allow sufficient time for deaeration (in compactors)	Modify input particle-size distribution
Causal and Opposing Effects		
van der Waals force	Cause vibration of the equipment (such as adding bouncing balls to prevent screen blinding) Use internal parts such as paddles or stirrers to break up aggregates	Consider using solid lubricants
Electrostatic force	Ground the equipment to reduce the effect of triboelectrification Install static eliminators (ionizers)	Modify feed moisture content
Capillary force	Induce *in-situ* evaporation of moisture Adjust the flow rate or temperature of drying gas to reduce the final moisture content	Modify solid/liquid separation unit to reduce moisture content of feed
Drag force	Adjust operating conditions affecting particle velocity (such as drum rotation speed or fluidizing gas velocity) Adjust the flow rate of the fluidizing gas Consider a different fluidizing gas Avoid fluidization by providing a means and allow sufficient time for deaeration	None
Compressive pressure	Adjust operating conditions affecting bed-agitation and collision frequency (such as mixer impeller speed, drum rotation speed, fluidizing gas velocity) Use different equipment configurations (such as compactor roller speed, gap between rollers) Consider a different type of unit	None
Adhesive and repulsive effects (in granulators)	Adjust operating conditions affecting bed-agitation and collision frequency Consider using a liquid binder with a different viscosity	None
Segregation potential	Avoid emptying the content of a batch mixer little by little Avoid bulk solids transfer where particles slide down a long, inclined chute Ensure mass flow in hoppers	Modify feed moisture content to affect cohesive forces Modify the PSD of the feed Use tangential entry of particles from pneumatic conveying lines
Limiting Values of Dimensionless Numbers		
Critical adhesion number	Adjust the flow rate or temperature of drying gas to reduce final moisture content Modify the amount of liquid binder	Modify solid/liquid separation unit to reduce moisture content of feed Modify impurity level and crystal habit in particle formation to affect surface roughness Modify surface roughness during milling
Critical compaction number	Manipulate adhesion forces (see above)	Modify input particle-size distribution
Critical flow number	Redesign the hopper with a different cone angle or opening Modify pressure distribution inside hopper by inserting a smaller hopper Coat the surface of the inclining wall with a different material	Modify solid/liquid separation unit to reduce moisture content of feed Consider using solid lubricants (a material with a different Hamaker constant)

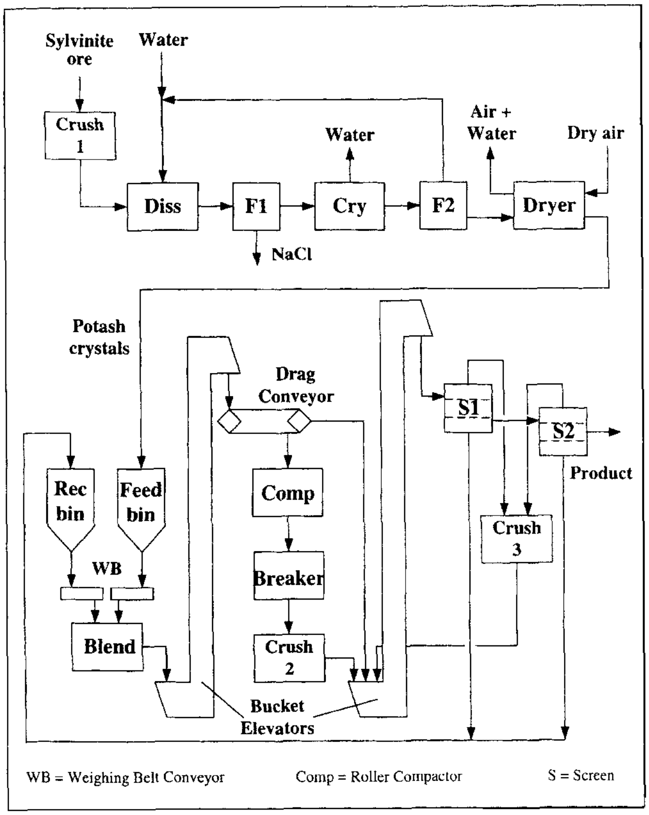

Figure 5. Potash process.

Based on the results of the analysis performed in Step 2, we can identify the key material or bulk properties and operating variables that should be modified. We can further develop an action plan, which may include modifications to the operating conditions or equipment design of the unit under consideration, as well as to those of an upstream unit. Table 9 lists the recommended actions to modify the causal and opposing effects in various situations. Some of them, especially those concerning solids flow and segregation, have been proposed in the literature (Carson et al., 1986: Johanson, 1978, 1987; Carson and Stuart-Dick, 1992; Stuart-Dick and Royal, 1992).

Example: Potash Plant

To illustrate this approach in obtaining useful relationships and practical solutions, we will now discuss an industrial example. Potash (KCl) is produced from sylvinite ore (mixture of KCl and NaCl). The flowsheet for this process is shown in Figure 5. Sylvinite ore is first crushed and then dissolved in hot water. Because of the joint solubility at a dissolving temperature, all the KCl dissolves while all of the NaCl remains as solid (Rajagopal et al., 1988). The latter is removed by passing the slurry through a filter (F1). KCl is then crystallized in a crystallizer (Cry) and removed in another filter (F2). These crystals are dried in a rotary dryer before entering the bulk solids processing step, the purpose of which is to obtain a product with suitable size for sale. In this example, some of the operational issues that may be encountered are discussed below. The parameter values for calculations are listed in Table 10.

Roller crusher (Crush 1)

Step 1. From Table 1 (item 3), we identify that insufficient or excessive breakage may be a problem. Excessive breakage is not an issue in this case, since the output of this crusher is sent to a dissolver. However, we want to avoid insufficient breakage because it may lead to incomplete dissolution, which causes KCl to be present as an impurity in the solid NaCl filter cake.

Step 2. The causal effect for breakage is the applied stress and the opposing effect is the material strength (Table 2). The minimum value of breakage number that leads to breakage can be estimated using Eq. 13, which gives the dependence of N_{Br} on N_{BI} shown in Figure 6a. For the system under consideration, the required pressure to break the particle as a function of size is depicted in Figure 6b. Since the critical size (associated with $N_{BI} = 16$) is estimated to be about

Table 10. Parameter Values for Potash Example

Properties of KCl	
Density, ρ_S	2,000 $kg\cdot m^{-3}$
Hamaker constant, A	6.6×10^{-20} J
Dielectric constant, ϵ_r	4.86
Electrical resistivity, Ω	10^{10} ohm·m
Young's modulus, E	2×10^{5} $N\cdot m^{-2}$
Surface fracture energy, γ_f	10^{4} $J\cdot m^{-2}$
Tensile strength, σ_t	8×10^{7} $N\cdot m^{-2}$
Yield strength, σ_y	8×10^{7} $N\cdot m^{-2}$
k (Eq. 20)	4×10^{-11} $m^{2}\cdot N^{-1}$
Angle of internal friction, ϕ	50°
Compressibility factor (for compaction)	10
Properties of Water	
Surface tension, γ	7.26×10^{-2} $N\cdot m^{-1}$
Viscosity, μ	10^{-3} $kg\cdot m^{-1}\cdot s^{-1}$
Properties of Air	
Density, ρ_F	1.3 $kg\cdot m^{-3}$
Viscosity, μ	1.8×10^{-5} $kg\cdot m^{-1}\cdot s^{-1}$
Roller Crusher	
Maximum particle size in outlet	1.6 mm
Average effective pressure	2.6×10^{6} $N\cdot m^{-2}$
Centrifugal Filter	
Magma density of feed	173 $kg\cdot m^{-3}$
Estimated cake porosity	0.365
Desired moisture content of the cake	15% (mass per mass of dry cake)
Rotary Dryer	
Feed dominant particle size	600 μm
Rotation speed, ω	6.5 $rad\cdot s^{-1}$
Roller Compactor	
Active roller width	50.8 mm
Gap between rollers	2.54 mm
Average pocket depth	7.62 mm
Recycle fraction of materials within nip	0.15
Nip angle	14°
Pneumatic Conveying System	
Bulk density during conveying, ρ_b	600 $kg\cdot m^{-3}$
Fluidizing gas	Air, relative humidity 10%
Gas velocity	3 $m\cdot s^{-1}$
Mean particle size	200 μm

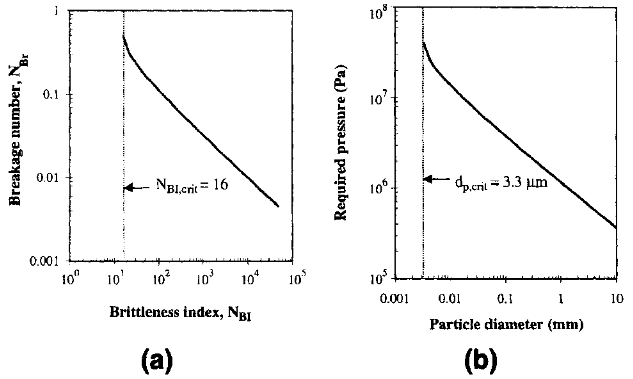

Figure 6. (a) Dependence of breakage number on brittleness index; (b) relationship between the required compressive pressure for breakage and particle size for the potash example.

3.3 μm, there is no problem in getting particles of the desired size (1.6 mm) through breakage. For particles of this desired size, $N_{BI} = 1.55 \times 10^4$ and the corresponding value of N_{Br}^* is 8×10^{-3}. This implies that the required pressure is about 6.4×10^5 N/m^2. The effective pressure in the roller crusher, estimated using a model proposed by Pietsch (1991), is 2.6×10^6 N/m^2 (Table 10). Since this is larger than the required pressure to cause breakage, we expect that there should not be a problem.

Step 3. If the applied force were not sufficient to cause breakage of the particles to below the specified maximum size, Table 9 could be used to propose some solutions. Obviously, an alternative is to manipulate the applied force. In reality, the magnitude of this force depends on equipment configurations and operating conditions. For example, in a roller crusher, it is determined by the roller diameter, gap between rollers, roughness of the roller surface, and the rotation speed. Depending on how large a change of force is required, changes such as replacing the roller or switching to another type of crusher may be considered.

Rotary dryer (Dry)

Step. 1. According to Table 1 (items 8, 12, and 27), there are three potential problems: entrainment caused by the flowing air, deposition of solids on the dryer wall, and formation of agglomerates in the upper section of the dryer where the particles are still wet. The corresponding responsible phenomena are fluidization, adhesion, and agglomeration, respectively. Steps 2 and 3 are followed to analyze each problem.

Entrainment Problem. Step 2. The causal effect is the drag force due to the blowing air, and the opposing effect is the gravity force (Table 2). We can calculate the fluidization number (Eq. 32) for various values of d_p and v_F, as depicted in Figure 7. If N_{Fl} is greater than unity, there is a good chance that the particle would be carried away by the flowing air. High air velocity can lead to higher drying rate, but on the other hand may cause entrainment problem. We expect that particles larger than about 400 μm in size would not be carried away even by air flowing at $v_F = 2$ m/s. Assuming an output PSD for an MSMPR crystallizer, it is expected that 98% (by mass) of the dry particles coming out of the dryer are larger than 200 μm in diameter. Therefore, the dry air velocity can be set as high as 1 m/s without significant entrainment.

Step 3. If entrainment were a problem, both Figure 7 and Table 9 suggest that the drying air velocity be reduced. Since the velocity cannot be reduced indefinitely and the presence of smaller particles is usually unavoidable, it is advisable to install a cyclone on the outlet gas line.

Deposition Problem. Step 2. For dry solids flowing by gravity through a rotary dryer, the potential adhesion forces are the van der Waals and electrostatic forces (due to triboelectrification). To prevent accumulation of charge on the wall, the equipment is usually grounded. The separation forces are mainly that of gravity and buoyancy. Drag force is not considered, since the dryer is operated under conditions where entrainment would not be a problem. Substituting appropriate expressions into Eq. 15, we get

$$N_{Ad} = \frac{A\eta}{4\pi(\rho_S - \rho_F) g d_p^2 z_0^2} \tag{36}$$

where η is the factor accounting for particle roughness, which is assumed to be 0.01 for an irregular-shaped KCl particle. We conclude from Eq. 36 that adhesion may occur when d_p is less than about 100 μm. Since the dominant particle size of the feed is 600 μm (Table 10), it is expected that deposition problem would not be severe for this case.

However, if the drying time is not sufficiently long, capillary force can be the dominant adhesive force. According to the general heuristics in Table 5, this occurs when the degree

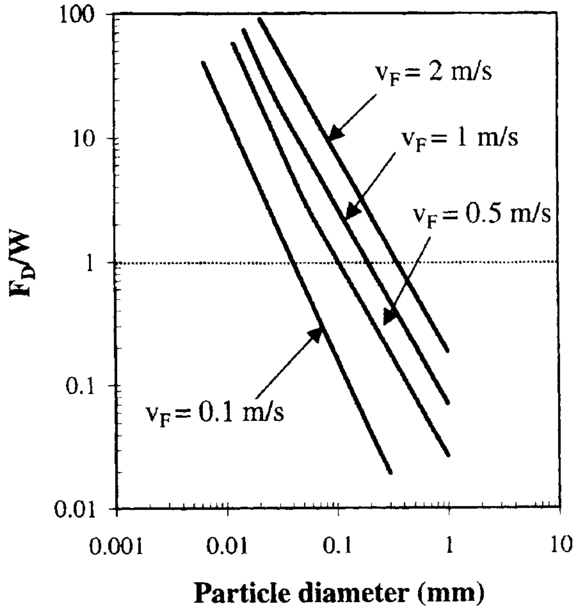

Figure 7. Ratio of drag force to gravity for various drying air velocity.

of saturation is between 0.4 to 0.8. Taking the maximum value for the capillary force, the adhesion number (Eq. 15) for this specific case is given by

$$N_{\mathrm{Ad}} = \frac{6\gamma}{(\rho_S - \rho_F) g d_p^2}. \tag{37}$$

In such a situation, the criterion for deposition is always satisfied, even for the largest particle in the stream (about 3 mm in diameter). This means a serious deposition problem may occur.

Step 3. Let us now look at possible solutions. Table 9 suggests that the final moisture content should be reduced by adjusting the flow rate or temperature of the drying gas, or by modifying the upstream solid/liquid separation unit. The excess feed moisture content can be a result of problems in the filtration and dewatering unit, which is located directly upstream from the dryer (Figure 5). Therefore, we will extend the analysis to the filter (F2).

Agglomeration Problem. Step 2. From Eqs. 17 and 18 in Table 6, we can predict that the coalescence probability increases if: (1) the particles are smaller; (2) initial velocity is lower; (3) the liquid is more viscous; (4) the liquid layer is thicker; or (5) the collision is less elastic. For particles in a rotary dryer, presumably assuming that the particle rotates at the same rate as the dryer, the particle initial velocity can be approximated as (Ennis et al., 1991)

$$u_0 = \frac{d_p \omega}{2} \tag{38}$$

where ω is the angular velocity. Assuming $N_{\mathrm{Ad}}^* = 1$, we obtain the maximum particle size above which coalescence does not occur is about 600 μm. This means agglomeration would reduce the number of particles less than 100 μm, thereby reducing the deposition problem. Since there is no foreseen problem, Step 3 is not performed.

Centrifugal filter (F2)

Step 1. Table 1 (items 2 and 17) suggests that low cake porosity may be a potential problem. Lower porosity leads to lower cake permeability, and therefore lower filtration rate (Hill and Ng, 1997). Under constant feed rate to the filter, material balance implies that a reduction in filtration rate leads to an increase in product moisture content. Thus, the problem of excessive moisture content can be related to the low porosity of the filter cake.

Step 2. The solids cake in the centrigual filter is continuously removed using a scraper. Since the scraper usually moves slowly, breakage is not expected to be important. For this reason, only the compaction issue will be pursued further in this example. According to Table 2, the causal effect for compaction is the compressive pressure on the filter cake. If compaction does not occur, it is estimated from the crystallizer PSD that the porosity of this cake is about 0.365 (Table 10). The total force acting on a particle in the layer of cake, which is the sum of the net centrifugal force and the drag force, can be expressed as

$$F_{\mathrm{tot}} = \frac{\pi}{6}(\rho_S - \rho_L) d_p^3 \omega^2 R + 3\pi\mu d_p v_F \tag{39}$$

where R is the radius of the centrifugal filter. Using Eq. 20, it is estimated that this force can cause a reduction in the cake porosity to 0.361. Furthermore, calculation results using a permeability model (MacDonald et al., 1991) and a filtration model (Svarovsky, 1981) show that the filtration rate decreases by about 1.4%. Material balance calculations reveal that this slight decrease causes the moisture content of the product to increase to 20%, which is significantly larger than the desired level of 15%.

Step 3. Clearly, the solution to this problem is to make sure that compaction is taken into account when designing the centrifuge. Another factor that has to be considered is the feed PSD, as it strongly affects the porosity. Manipulating the feed PSD is an alternative solution (Table 9). Since the filter receives its feed from a crystallizer (Cry), controlling the PSD of the crystals formed in the crystallizer can be advantageous. Furthermore, fluctuation of the feed PSD must also be considered. This can occur, for example, because of the reworking of off-specification crystals. These crystals are dissolved and sent back to the crystallizer, thus creating occasional fluctuations in the crystallizer feed, which in turn affects the PSD. The worst case, in which the porosity is the smallest, must be taken as the basis for design.

Feed bin

Step 1. From Table 1 (items 20 and 21), plugging and erratic flow are some of the potential problems in storage bins. Plugging can be caused by the formation of a mechanical arch at the hopper outlet, which prevents the material from flowing. Another potential problem is in-bin segregation.

Step 2. As Table 6 indicates, the problem of solids flow can be assessed using the flow number (Eq. 22). This expression shows that for a given hopper, the flow property of bulk solids depends on the particle size (d_p) and the adhesion force (F_{adh}). If the particles from the rotary dryer are slightly wet, the bin can be plugged due to the strong capillary force. Equally important is the design of the bin and the material characteristics, as pointed out by Carson and Marinelli (1994). Using Eq. 31, along with a predicted value of N_{Fw}^*, we can calculate the minimum outlet diameter above which mass flow would occur, as depicted in Figure 8. Due to savings in overall headroom and the cost of elevating material into the bin, it is often desired to have shallow sliding walls (large β) (Marinelli and Carson, 1992). As β increases, the corresponding value of N_{Fw}^* also increases.

Segregation may be a problem since the feed PSD is quite wide, and it can be accentuated if funnel flow occurs (heuristics related to segregation in Table 5). Changing to mass flow would minimize, but not completely eliminate segregation problem. For this example, segregation may still occur to a slight extent, but is not a real concern because of the presence of a blender (Blend) downstream.

Step 3. If problems do occur, Table 9 proposes some solutions. As Eq. 22 indicates, the flow number increases if the

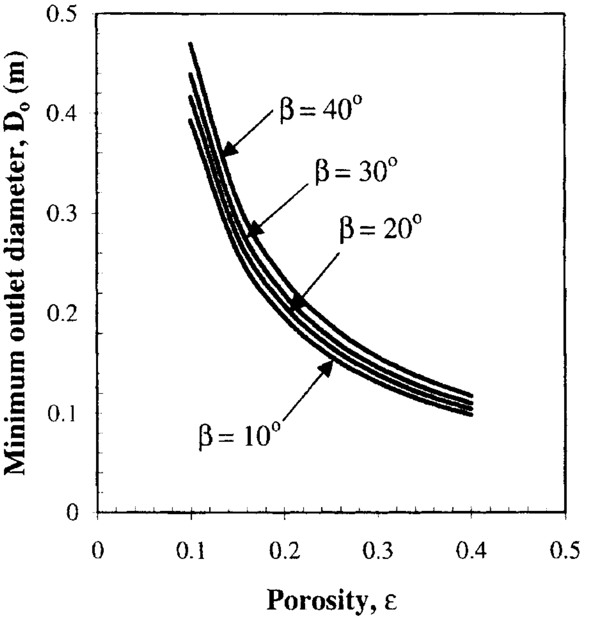

Figure 8. Minimum bin outlet diameter for various values of half-cone angle and porosity.

porosity of the material is higher or the particles are larger. For the potash process, we can consider modifying the feed PSD of the crystals from the crystallizer. Alternatively, adhesion forces should be minimized. The most obvious way is to make sure that the feed enters the bins in a dry condition. If the particles are cohesive even in a dry condition, it may be useful to introduce a lubricant that has a lower Hamaker constant, causing the van der Waals force to decrease.

If the flow number cannot be improved, the appropriate action is to modify the equipment design to allow mass flow. There are three interesting solutions (Table 9). First, the bin can be replaced with a new unit having a steeper conical section (small β). The major drawback is the need for a taller unit. The second option is to reduce wall friction by coating or replacing the hopper interior with another material. The third option is to use a smaller but steeper bin inserted into the existing unit (for example, the BINSERT system patented by Jenike and Johanson, Inc.). Properly designed, the cone-in-cone design allows mass flow to occur. The last option seems to be the most favorable for retrofitting, since it only requires a minor modification to the existing unit.

Roller compactor (comp)

Step 1. Let us focus on product strength, which is suggested as one of the problems in a size enlargement unit (Table 1, item 18). In a compactor, a mass of powder is shaped and densified by applying a compressive force. As discussed previously, there is a limiting value of compressive force that produces a structure with sufficient strength, which will not break readily upon further processing.

Step 2. According to Table 6, the dimensionless number to consider is the compaction number N_{Co}. Figure 9a shows the dependence of the critical compaction number (N_{Co}^*) on the desired product strength for different values of initial porosity and adhesive forces among the particles, calculated using Eqs. 20 and 21. We can see that a low initial porosity leads to a lower N_{Co}^*, but the effect is not very pronounced at high values of N_{SI}. At a constant compression, an increase in ϵ_0 leads to a decrease in the resulting agglomerate strength.

Step 3. Porosity can be modified by manipulating input PSD (Table 9). To ensure low initial porosity, the PSD of the feed must be wide. For this reason, the feed is premixed with recycle streams containing fine particles. To avoid variation in bulk porosity, segregation in preceding units must be strictly avoided. Table 9 also suggests that air entrapment should be avoided by providing enough time for deaeration. This can be done, for example, by adjusting the roller speed in a roller compactor. Since the applied compressive pressure on the material depends on the equipment configuration and operating conditions, the equipment must be designed properly to yield the desired compressive pressure. Some empirical models relating compressive pressure to equipment design and operating variables are available. Pietsch (1991) related the maximum compressive pressure in a roller compactor to the precompaction pressure, roller speed, gap between rolls, and material characteristics. Figure 9b shows the effect of roller diameter on the compressive pressure for this system, using his correlation. Sometimes particle breakage occurs upon compression. To some extent, this is favorable since lower d_p also leads to a higher N_{SI}.

An alternative solution is to increase N_{SI} by adding a solid binder which can increase the adhesion forces between the particles. Figure 9a shows that the more cohesive materials (that is, higher F_{adh}) require lower compressive pressure to achieve the same strength. Since the adhesion force is mainly the van der Waals force, Eq. 7 shows that a soft material with a high Hamaker constant is a good candidate for this purpose.

Screens (S1 and S2)

Step 1. Percolation of small particles and screen blinding due to adhesion are two major potential problems in screen-

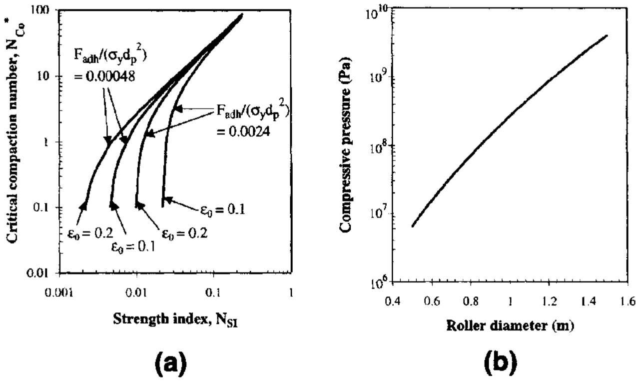

Figure 9. (a) Relationship between compaction number and strength index; (b) required applied pressure for compaction as a function of roller diameter.

ing (Table 1, items 9 and 30). This causes near-cut-size particles to overflow.

Step 2. As suggested by Table 2, the causal effect for segregation is bulk motion. Percolation occurs because when the screen vibrates, smaller particles move down through the gaps between larger particles (Williams, 1990). Also, if the mixture consists of particles of different substances, light particles move upward. Uniformity is considered to be the opposing effect since if the particles were all of the same size and density, segregation would not occur. Screen blinding can be a result of plugging or wedging, where near-cut-size particles block the apertures. Another possible cause is adhesion of small particles on the apertures due to van der Waals force.

Step 3. There are several options to eliminate these problems (Table 9). Percolation can be minimized by operating the screen in such a way that there is only a thin layer of particles on the surface of the screen. It can be achieved, for example, by changing the inclination of the screen. The problem of screen blinding can often be resolved by increasing vibration frequency or amplitude, or by installing bouncing rubber balls on a deck placed below the screen (Matthews, 1971). Another possible remedy is by heating the screen to cause *in-situ* evaporation, which is appropriate if the cohesiveness is mainly caused by moisture (Beddow, 1981).

Pneumatic conveying line

Step 1. Pneumatic conveying is used to transport the undersized particles from the screens to the recycle bin. Potential problems are attrition, solids deposition, and formation of aggregates (Table 1, items 6, 11, 16 and 29). However, agglomeration is not a real concern here because the pneumatic line feeds the recycle bin, whose output goes to the ribbon blender. The agglomerates are expected to break due to agitation in the blender. Therefore, although agglomeration does occur, it is not expected to cause a disturbance to the process.

Step 2. The high velocity of particles transported in a pneumatic line leads to possible breakage, especially in dilute-phase conveying. The situation can be described simplistically using the model depicted in Figure 4b. Using Eq. 26, it is estimated that the impact pressure is only about 2,700 Pa. This corresponds to $N_{Br} = 3.4 \times 10^{-5}$, much less than the limiting value predicted using Eq. 13 for potash particles with a diameter of 200 μm. Thus, particle attrition may not be of real concern.

To assess the possibility of deposition, we compare the adhesive and separating forces. Moisture is not likely to cause a problem in this system, since the relative humidity is very low. Taking van der Waals force as the primary adhesion force and drag force to be the separating force, the expression for the adhesion number becomes

$$N_{\mathrm{Ad}} = \frac{A\eta}{3\pi\rho_F d_p z_0^2 f(N_{Re})}. \tag{40}$$

Using appropriate expression for $f(N_{Re})$ (Bird et al., 1960) and assuming $\eta = 0.01$, we obtain that the adhesion number is less than unity. Thus, adhesion problem due to van der Waals force is not significant. However, it should be checked whether or not electrostatics creates a problem. Although the equipment is grounded, a charge may still accumulate in the particles if they are good insulators (general heuristics in Table 5). For potash particles with a diameter of 200 μm, the actual magnitude of the electrostatic force generated (assumed to be 60% of its maximum value calculated from Eq. 5) is almost four order of magnitudes higher compared to the particle weight. Fortunately, the relaxation time is only about 0.4 s, indicating that the electrostatic force is practically unimportant.

Step 3. Had there been any problem related to triboelectrification occurring in the pneumatic line, some preventive action depicted in Table 9 would have been appropriate. For example, static eliminators such as an ionizer may be installed. Increasing humidity by introducing steam can also reduce the electrostatic effect. However, since condensation of the steam may lead to increased moisture content, it may introduce other problems (such as encrustation and plugging) rather than just eliminating the issue of concern.

Conclusions

To date, the powder technology community has focused primarily on studying fundamental phenomena. Systematic and holistic approach to the design of a complete solids processing plant has received scant attention. This is a serious omission for two reasons. First, experience shows that a solids plant can fail spectacularly (Merrow, 1985). Frequently, this was not because the fundamental phenomenon causing the problem was not known; rather, we failed to ferret out the problem at the stage of conceptual design. Second, globalization engenders relentless pressure to shorten the time-to-market in chemical processing industries. It used to take ten years or so to build a large-scale grassroots chemical plant starting from basic chemistry. Most companies are now aiming for four to five years. A systematic, fundamental-based approach is essential for reliable, quick response. Indeed, approaches and techniques in systems engineering have been firmly established for the design of complete gas-liquid plants (Douglas, 1988; Biegler et al., 1997; Seider et al., 1998). It is critical that design and engineering science of solids processes be tightly integrated.

As part of this overall goal, we have presented a method for resolving operational problems in solids processing plants, the entirety of which is depicted in Figure 10. It takes into account the effects of both continuum and particle-scale phenomena, while keeping an integral view of the whole process. Using a three-step procedure, the problems are identified and classified according to the responsible phenomena. By relating the problem to material properties, particle attributes, and interparticle forces, we systematically seek possible solutions. The method allows the user to predict the performance of a new process in the synthesis phase (forecasting), resolve operation problems (troubleshooting), and make improvements to an existing process (retrofitting). This framework is not a stand-alone tool. Rather, its intent is to help systematize tasks for resolving operational problems.

In fact, not all relevant phenomena are enumerated for a given potential problem. For example, a more realistic analy-

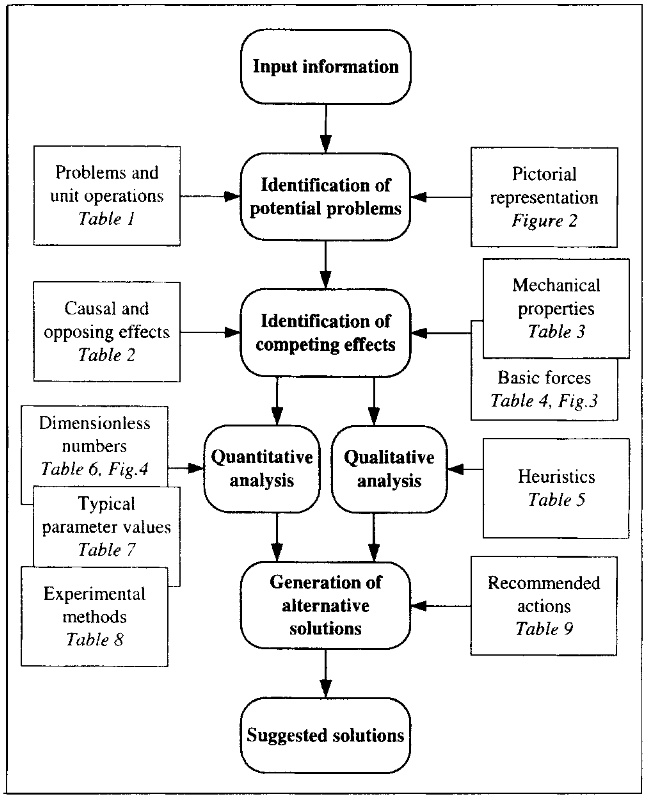

Figure 10. Systematic method to identify and resolve operational problems in solids processing.

sis of particle capture would involve not only the attractive forces, but also the various hydrodynamic forces as well as Brownian motion (Payatakes et al., 1974a,b; Tien and Payatakes, 1979). The presence of polyelectrolytes can also significantly affect adhesion. Although only simplified models are considered, the derived equations can be used to point to the right direction for necessary actions, and identify the need for experimental data. For example, the expression for the flow number (Eq. 22) reflects the dependence of flow behavior on material properties and operating variables. While its value cannot be accurately estimated with the simple model for adhesion forces, it shows the correct dependence on particle size and porosity. These parameters can be properly manipulated to get the desired behavior. Obviously, this framework can readily accept more rigorous models and detailed analysis to improve the predictions.

We did not consider the operational issues related to crystallization in this article. In reality, controlling the product quality in a crystallizer has a significant impact on the process. It has been shown in the examples that a different crystal PSD might have eliminated a number of possible problems, such as deposition in a dryer, erratic flow in a bin, and low product strength in a compactor. Therefore, our future plan is to extend the method to include crystallization. Of equal importance is to integrate this method with the synthesis method for bulk solids processing systems (Wibowo and Ng, 1999). It is far better to eliminate potential operational problems in the original design than to retrofit a plant when difficulties arise. Efforts in this direction are underway.

Acknowledgment

We express our appreciation to the National Science Foundation, Grant No. CTS-9908667, for support of this research.

Notation

A = Hamaker constant, J
CE = causal effect
d_p = representative particle size or diameter, m
D = hopper diameter, m
D_o = hopper outlet diameter, m
e = coefficient of restitution, dimensionless
E = Young's modulus, $N \cdot m^{-2}$
f_c = unconfined yield stress, $N \cdot m^{-2}$
ff = flow factor, dimensionless
F_{adh} = adhesion force, N
F_B = buoyancy force, N
F_C = capillary force, N
F_D = drag force, N
F_E = electrostatic force, N
F_{sep} = separating force, N
F_{vdW} = van der Waals force, N
g = gravitational constant, $m \cdot s^{-1}$
h = height, m
H = material hardness, $N \cdot m^{-2}$
k = Janssen constant, dimensionless
k = constant (in Eq. 20), $m^2 \cdot N^{-1}$
N = dimensionless number
N_{Ad} = adhesion number, dimensionless
N_{BI} = brittleness index, dimensionless
N_{Br} = breakage number, dimensionless
N_{Co} = compaction number, dimensionless
N_{Fl} = fluidization number, dimensionless
N_{Fw} = flow number, dimensionless
N_{Re} = Reynolds number, dimensionless
N_{SI} = strength index, dimensionless
OE = opposing effect
p = pressure, $N \cdot m^{-2}$
q = charge, C
r = dimension of surface asperities, m
t_r = retention time, s
u_0 = initial particle velocity, $m \cdot s^{-1}$
v_F = fluid velocity, $m \cdot s^{-1}$
v_P = particle velocity, $m \cdot s^{-1}$
W = particle weight, N
z = separation distance, m
z_0 = constant, 4×10^{-10} m

Greek letters

β = half-cone angle of a hopper, degrees
γ = surface tension of liquid, $N \cdot m^{-1}$
γ_f = surface fracture energy, $J \cdot m^{-2}$
δ = thickness of liquid layer, m
ϵ = porosity, dimensionless
ϵ_r = dielectric constant, dimensionless
ϵ_0 = permittivity of vacuum = 8.85×10^{-12} $C \cdot m^{-2}$
η = ratio between the dimension of asperities and particle diameter
θ = wetting angle, degrees
θ = angle of approach (Eq. 26), degrees
μ = viscosity, $kg \cdot m^{-1} \cdot s^{-1}$
μ_w = coefficient of wall friction, dimensionless
ρ = density, $kg \cdot m^{-3}$
σ_c = compressive pressure, $N \cdot m^{-2}$
σ_t = tensile strength, $N \cdot m^{-2}$
σ_y = yield strength, $N \cdot m^{-2}$
ϕ = angle of internal friction, degrees
ϕ_w = angle of wall friction, degrees
ψ = filling angle
Ω = electrical resistivity, ohm·m
ω = angular velocity, $rad \cdot s^{-1}$

Subscripts

b = bulk
F = fluid
L = liquid
S = solid (or solid in vacuum)
SL = solid in the presence of liquid
v = vertical
0 = initial
$*$ = limiting value

Literature Cited

Ashby, M. F., and D. R. H. Jones, *Engineering Materials: An Introduction to Their Properties and Applications*, Pergamon Press, Oxford (1980).

Bailey, A. G., "Electrostatic Phenomena during Powder Handling," *Powder Technol.*, **37**, 71 (1984).

Barton, G. W., and J. D. Perkins, "Experiences with SPEEDUP in the Mineral Processing Industries," *Chem. Eng. Res. Des.*, **66**, 408 (1988).

Beddow, J. K., "Dry Separation Techniques," *Chem. Eng.*, **88**(16), 70 (1981).

Berry, D. A., and K. M. Ng, "Synthesis of Crystallization-Distillation Hybrid Separation Processes," *AIChE J.*, **43**, 1751 (1997).

Biegler, L. T., I. E. Grossmann, and A. W. Westerberg, *Systematic Methods of Chemical Process Design*, Prentice Hall, Upper Saddle River, NJ (1997).

Bird, R. B., W. E. Stewart, and E. N. Lightfoot, *Transport Phenomena*, Wiley, New York (1960).

Carson, J. W., T. A. Royal, and D. J. Goodwill, "Understanding and Eliminating Particle Segregation Problems," *Bulk Solids Handling*, **6**, 139 (1986).

Carson, J. W., and J. Marinelli, "Characterize Bulk Solids to Ensure Smooth Flow," *Chem. Eng.* **101**(4), 78 (1994).

Carson, J. W., and D. Stuart-Dick, "Retrofits Can Correct Flow Problems," *Bulk Solids Handling*, **12**, 245 (1992).

Chang, W.-C., and K. M. Ng, "Synthesis of Processing System Around a Crystallizer," *AIChE J.*, **44**, 2240 (1998).

Cisternas, L. A., and D. F. Rudd, "Process Designs for Fractional Crystallization from Solution," *Ind. Eng. Chem. Res.*, **32**, 1993 (1993).

Dahneke, B., "The Capture of Aerosol Particles by Surfaces," *J. Colloid Interf. Sci.*, **37**, 342 (1971).

Dahneke, B., "The Influence of Flattening on the Adhesion of Particles," *J. Colloid Interf. Sci.*, **40**, 1 (1972).

Davies, D. K., "Electrostatic Problems in Powder Handling," *Bulk 2000: Bulk Material Handling Towards the Year 2000*, Mechanical Engineering Publications, Bury St. Edmunds, Suffolk, U.K. (1991).

Douglas, J. M., *Conceptual Design of Chemical Processes*, McGraw-Hill, New York (1988).

Eichel, F. G., "Electrostatics," *Chem. Eng.*, **74**(6), 153 (1967).

Ennis, B. J., G. I. Tardos, and R. Pfeffer, "A Microlevel-based Characterization of Granulation Phenomena," *Powder Technol.*, **65**, 257 (1991).

Geldart, D., "Types of Gas Fluidization," *Powder Technol.*, **7**, 285 (1973).

Hill, P. J., and K. M. Ng, "Simulation of Solids Processes Accounting for Particle-Size Distribution," *AIChE J.*, **43**, 715 (1997).

Hixon, L. M., "Select an Effective Size-Reduction System," *Chem. Eng. Prog.*, **87**(5), 36 (1991).

Janssen, H. A., "Versuche über Getreidedruck in Silozellen," *Zeit. Ver. Deutsch. Ing.*, **39**, 1045 (1895).

Jenike, A. W., "Storage and Flow of Solids," Bulletin No. 123, Utah Engineering Experimentation Station, University of Utah, Salt Lake City, UT (1964).

Johanson, J. R., "Particle Segregation and What To Do About It," *Chem. Eng.*, **85**, 183 (1978).

Johanson, J. R., "Solids Segregation—Case Histories and Solutions," *Bulk Solids Handling*, **7**, 205 (1987).

Johanson, J. R., "The Johanson Indicizer™ System vs. the Jenike Shear Tester," *Bulk Solids Handling*, **12**, 237 (1992).

Johanson, J. R., and K. D. Johanson, "Improve Your Solids Processing," *Chem. Eng.*, **95**, 77 (1988).

Jones, G. L., "Simulating the Effects of Changing Particle Characteristics in Solids Processing," *Comput. Chem. Eng.*, **8**, 329 (1984).

Kendall, K., "The Impossibility of Comminuting Small Particles by Compression," *Nature*, **272**, 710 (1978).

Krupp, H., "Particle Adhesion: Theory and Experiment," *Adv. Colloid Interf. Sci.*, **1**, 111 (1967).

Lee, R. J., and L. S. Fan, "The Effect of Solid Interaction Forces on Pneumatic Handling of Sorbent Powders," *AIChE J.*, **39**, 1018 (1993).

Lide, D. R., ed., *CRC Handbook of Chemistry and Physics*, 78th ed. 1997/1998, CRC Press, Boca Raton, FL (1997).

MacDonald, M. J., C. F. Chu, P. P. Guilloit, and K. M. Ng, "A Generalized Blake-Kozeny Equation for Multisized Spherical Particles," *AIChE J.*, **37**, 1583 (1991).

Marinelli, J., and J. W. Carson, "Solve Solids Flow Problems in Bins, Hoppers, and Feeders," *Chem. Eng. Prog.*, **88**(5), 22 (1992).

Matthews, C. W., "Screening," *Chem. Eng.*, **78**(4), 99 (1971).

Merrow, E. W., "Linking R&D to Problems Experienced in Solids Processing," *Chem. Eng. Prog.*, **81**(5), 14 (1985).

Molerus, O., "Effect of Interparticle Cohesion Forces on the Flow Behaviour of Powders," *Powder Technol.*, **20**, 161 (1978).

Molerus, O., "Interpretation of Geldart's Type A, B, C and D Powders by Taking Into Account Interparticle Cohesion Forces," *Powder Technol.*, **33**, 81 (1982).

Moyers, C. G., "Don't Let Dryer Problems Put You Through the Wringer," *Chem. Eng. Prog.*, **88**(12), 34 (1992).

Nelson, R. D. Jr., *Dispersing Powders in Liquids*, Elsevier, Amsterdam (1988).

Ouchiyama, N., and T. Tanaka, "Porosity Estimation for Random Packings of Spherical Particles," *Ind. Eng. Chem. Fundam.*, **23**, 490 (1984).

Payatakes, A. C.., C. Tien, and R. M. Turian, "Trajectory Calculation of Particle Deposition in Deep Bed Filtration: Part I. Model Formulation," *AIChE J.*, **20**, 889 (1974a).

Payatakes, A. C., C. Tien, and R. M. Turian, "Trajectory Calculation of Particle Deposition in Deep Bed Filtration: Part II. Case Study of the Effect of Dimensionless Groups and Comparison with Experimental Data," *AIChE J.*, **20**, 900 (1974b).

Pietsch, W., *Size Enlargement by Agglomeration*, Wiley, Chichester, U.K.; Otto Salle Verlag, Frankfurt/M, Germany; and Verlag Sauerländer AG, Aarau, Germany, (1991).

Pietsch, W., "Successfully Use Agglomeration for Size Enlargement," *Chem. Eng. Prog.*, **92**(4), 29 (1996).

Pietsch, W., "Granulate Dry Particulate Solids by Compaction and Retain Key Powder Properties," *Chem. Eng. Prog.*, **93**(4), 24 (1997).

Pressly, T. G., and K. M. Ng, "Process Boundary Approach to Separations Synthesis," *AIChE J.*, **45**, 1939 (1999).

Quinn, J. B., and G. D. Quinn, "Indentation Brittleness of Ceramics: A Fresh Approach," *J. Mat. Sci.*, **32**, 4331 (1997).

Rajagopal, S., K. M. Ng, and J. M. Douglas, "Design of Solids Processes: Production of Potash," *Ind. Eng. Chem. Res.*, **27**, 2071 (1988).

Rajagopal, S., K. M. Ng, and J. M. Douglas, "A Hierarchical Procedure for the Conceptual Design of Solids Processes," *Comput. Chem. Eng.*, **16**, 675 (1992).

Rossiter, A. P., and J. M. Douglas, "Design and Optimisation of Solids Processes: 1. A Hierarchical Decision Procedure for Process Synthesis of Solids Systems," *Chem. Eng. Res. Dev.*, **64**, 175 (1986a).

Rossiter, A. P., and J. M. Douglas, "Design and Optimisation of Solids Processes: 2. Optimisation of Crystalliser, Centrifuge, and Drying Systems," *Chem. Eng. Res. Dev.*, **64**, 184 (1986b).

Rouault, Y., and S. Assouline, "A Probabilistic Approach towards Modeling the Relationships between Particle and Pore Size Distributions: The Multicomponent Packed Sphere Case," *Powder Technol.*, **96**, 33 (1998).

Rumpf, H., "Zur Theorie der Zugfestigkeit von Agglomeraten bei Kraftüberagung an Kontaktpunkten," *Chem. Ing. Tech.*, **42**, 538 (1970).

Schönert, K., "The Role of Fracture Physics in Understanding Comminution Phenomena," *Trans. SME/AIME*, **252**, 21 (1972).

Schubert, H., "Capillary Forces—Modeling and Application in Particulate Technology," *Powder Technol.*, **37**, 105 (1984).

Seider, W. D., J. D. Seader, and D. R. Lewin, *Process Design Principles: Synthesis, Analysis and Evaluation*, Wiley, New York (1998).

Shackelford, J. F., ed., *The CRC Material Science and Engineering Handbook*, CRC Press, Boca Raton, FL (1992).

Sommer, K., "Size Enlargement," *Ulmann's Encyclopaedia of Industrial Chemistry*, 5th ed., vol. B2, Weinheim, Germany (1988).
Stuart-Dick, D., and T. A. Royal, "Design Principles for Chutes to Handle Bulk Solids," *Bulk Solids Handling*, **12**, 447 (1992).
Svarovsky, L., ed., *Solid-Liquid Separation*, 2nd ed., Butterworths, London (1981).
Tardos, G. I., "High and Low Shear Granulation of Fine Powders—A Review," Paper 264a, AIChE Meeting, Miami Beach, FL (1998).
Tardos, G. I., Personal notes (1999).
Tien, C., and A. C. Payatakes, "Advances in Deep Bed Filtration," *AIChE J.*, **25**, 737 (1979).
Tombs, T. N., "Electrostatic Force on a Moist Particle Near a Ground Plane," *J. Adhesion*, **51**, 15 (1995).
van Vlack, L. H., *Elements of Materials Science and Engineering*, 4th ed., Addison-Wesley, Reading, U.K. (1980).
Visser, J., "On Hamaker Constants: A Comparison between Hamaker Constants and Lifshitz-van der Waals Constants," *Adv. Coll. Interface Sci.*, **3**, 331 (1972).
Visser, J., "Adhesion of Colloidal Particles," *Surface and Colloid Science*, Vol. 8, E. Matijevic, ed., Wiley, New York (1976).
Visser, J., "An Invited Review: Van der Waals and Other Cohesive Forces Affecting Power Fluidization," *Powder Technol.*, **58**, 1 (1989).
Wibowo, C., and K. M. Ng, "Synthesis of Bulk Solids Processing Systems," *AIChE J.*, **45**, 1629 (1999).
Wibowo, C., and K. M. Ng, "Unified Approach for Synthesizing Crystallization-Based Separation Processes," *AIChE J.*, **46**, 1400 (2000).
Williams, J. C., "Mixing and Segregation in Powders," *Principles of Powder Technology*, M. Rhodes, ed., Wiley, Chichester, p. 71 (1990).
Woodcock, C. R., and J. S. Mason, *Bulk Solids Handling*, Blackie Academic & Professional, London (1987).
Young, K. F., and H. P. R. Frederikse, "Compilation of the Static Dielectric Constant of Inorganic Solids," *J. Phys. Chem. Ref. Data*, **2**, 313 (1973).

Manuscript received Mar. 10, 2000, and revision received June 7, 2000.